SCIENCE CHINA
Technological Sciences

•Article•

November 2018 Vol.61 No.11: 1666–1678
https://doi.org/10.1007/s11431-017-9204-y

Interpolation-based contour error estimation and component-based contouring control for five-axis CNC machine tools

LI XiangFei, ZHAO Huan*, ZHAO Xin & DING Han

State key Laboratory of Digital Manufacturing Equipment and Technology, Huazhong University of Science and Technology, Wuhan 430074, China

Received October 9, 2017; accepted January 18, 2018; published online March 21, 2018

High accuracy contour error estimation and direct contour error control are two major approaches to reduce the contour error. However, two key factors make them complex for five-axis machine tools: the nonlinear kinematics and the coupling between the tool position and orientation. In this study, by finding the reference point nearest to the current actual position, and interpolating the point with two neighboring reference points and using the distance ratio, a new contour error estimation method for five-axis machine tools is proposed, which guarantees high accuracy while depending on only the reference points. By adding a weighted contour error on the tracking error in the workpiece coordinate system, and specifying a desired second-order error dynamics based on the error variable, an effective contouring control method is proposed, which can alleviate the problem: when the contour error components are introduced into the controller, the contour errors increase instead in some regions of the tracking trajectory. A series of experiments are performed on a tilting-rotary-table (TRT) type five-axis machine tool. The results reveal that the proposed estimation method has high accuracy, and compared with the case without contour error control, the proposed control approach can reduce the contour error along the whole trajectory.

five-axis, contour error, contouring control, interpolation, component-based

Citation: Li X F, Zhao H, Zhao X, et al. Interpolation-based contour error estimation and component-based contouring control for five-axis CNC machine tools. Sci China Tech Sci, 2018, 61: 1666–1678, https://doi.org/10.1007/s11431-017-9204-y

1 Introduction

Five-axis CNC machine tools, which include three translational and two rotary drives, have the ability to follow free-form surfaces with required geometry and dimensional accuracy. Therefore, they have been extensively utilized in the manufacturing application fields. However, during the five-axis contouring operation, the individual servo tracking lag [1] and the unmatched dynamic responses among different axes [2] are always inevitable. The resulting tracking errors are transferred kinematically to the tool tip position and the tool orientation, resulting in the contour errors between the desired and the actual contours. They must be controlled to avoid violating the tolerance of the product. To reduce the contour error, which is defined as the shortest distance of the actual position from the reference contour [3], considerable research efforts have been utilized to come up with a range of solutions over the past few decades, and the proposed approaches concentrate mainly on estimating the contour error accurately and designing the contouring controller effectively.

The first attempt was made by Koren [4] for biaxial machining, where the contour error is estimated as linear relationships of tracking errors. For arbitrary curves, by adopting the spatial contour error, a contour error estimation method was proposed by Yeh and Hsu [5], where contour error can be acquired from the actual tool position to the tangent line at the reference position. Using point-to-curve

* Corresponding author (email: huanzhao@hust.edu.cn)

distance function, Zhu et al. [6] presented a second-order approach for the contour error estimations of arbitrary trajectories. By adopting the distance from the actual position to the local approximate circle of the desired curve, Yang and Li [7] acquired the contour errors of arbitrary smooth tool paths. By using the average direction of the reference and actual tool velocities, Chuang and Liu [8] provided a linear approximation method to estimate the contour error for multi-axis machine tools. For three-dimensional machining operations, based on the instantaneous curvature of the reference curve, El Khalick and Uchiyama [9] obtained the contour error iteratively. By decoupling the tracking error into the tangential and normal errors in the local task coordinate frame, the normal error was used as the approximation of contour error by Chiu and Tomizuka [10]. Based on the canonical approximation, Shi and Lou [11] proposed a novel contour error estimation approach for three-dimensional contouring control. The approximation is obtained locally from the Taylor expansion of the reference contour. In contrast to the local task coordinate frame, for biaxial systems Yao et al. [12] provided a global task coordinate frame (GTCF), by which the contour error can be acquired as the first order approximation of the true contour error. Later, a similar contour error estimation was provided by Wu et al. [13] in biaxial systems. For estimating the contour error more accurately, by adopting the line-segment approximation of the desired curve with n number of the reference positions, a contour error estimation approach for arbitrary tool paths was presented by Erkorkmaz and Altintas [14]. Subsequently, a similar approach was provided by Huo et al. [15], where its inputs are a series of the actual positions as well as the desired positions of the machine tool. Utilizing the polynomial root-seeking formulae, an essentially exact contour error calculation approach was provided by Conway et al. [16]. Differing from the above studies, a concept of equivalent contour error was proposed for arbitrary smooth tool paths by Chen and Wu [17]. The equivalent errors, which consist of equivalent contour errors and tangential error, are taken as the control objective. Ghaffari and Ulsoy [18] proposed a dynamic contour error estimation (CEE) method based on the Newton update algorithm. Because the convergence rate of the Newton update algorithm is independent of the desired contour, the proposed CEE is almost identical to the true contour error for the sharp corners or different feedrates.

The contour error estimations for biaxial and triaxial machining operations have been fully studied. However, one key factor limits their direct application to five-axis machine tools, that is, the five-axis contouring accuracy is affected simultaneously by the tool tip position and the tool orientation, as illustrated in Figure 1. For five-axis machine tools, the contour errors can be classified into two categories. One is the tool tip contour error ε_P, which is considered as the shortest distance of the actual tool tip from the reference position trajectory, the other is the tool orientation contour error ε_O, which is regarded as the orthogonal angular deviation of the actual tool orientation from the reference orientation trajectory. Lo [19] presented a five-axis contour error estimation approach, where the tool tip contour error is acquired by the projections of tracking error, and the tool orientation contour error is obtained by using two rotational angles. Sencer et al. [1] provided an estimation approach, by which the tool tip contour error can be approximated adopting the projections of tracking error in the shifted Frenet frame, and the tool orientation contour error can be acquired using a vector. The vector is obtained by transforming the tool orientation tracking error. However, since the tool tip and tool orientation contour errors are independently estimated, large overcut or undercut may be caused in the machined surface. In order to solve this problem, El Khalick and Uchiyama [20] provided a new tool orientation contour error estimation method, where the tool orientation used for the orientation contour error estimation is synchronized to the tool tip position. Zhang et al. [21] presented an off-line approach to predict the contour errors analytically for five-axis splined paths, where the tool tip contour error is estimated by searching numerically the point nearest to the actual tool tip position, and the tool orientation contour error is acquired in a similar way. However, the estimation performance may degrade when the adopted models are not accurate. Yang and Altintas [22] proposed a generalized on-line estimation approach for five-axis CNC machine tools, where the corresponding axis components of contouring errors are obtained by the drive commands and the generalized Jacobian. In our previous work [23], a new estimation method was proposed, where the tool tip contour error estimation is based on the second-order Taylor series expansion, while the tool orientation contour error estimation is obtained by the linear interpolation method. However, it depends on the geometrical information of the desired contour, which may increase the computational load.

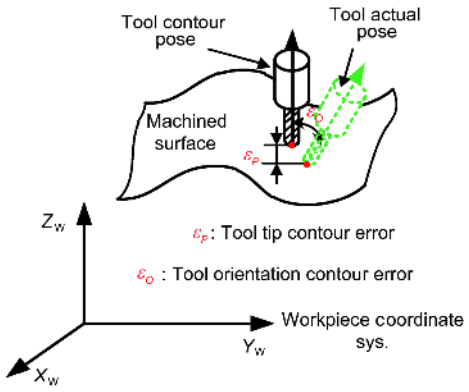

Figure 1 (Color online) Five-axis contour error definition.

In addition to the accurate estimation of the contour error, effective contouring controller design is also crucial to reduce the contour error. Two major control methods are frequently used. The first method is the tracking control, where the reduction of contour error is achieved indirectly by reducing the tracking error. Some tracking controllers such as zero phase error tracking controller (ZPETC) [24], feedforward controller [25] and sliding mode controller (SMC) [26] can improve the tracking accuracy. However, for multi-axis motion systems, high tracking accuracy does not necessarily mean good contouring accuracy [27]. Thus, the second method, called the contouring control, is to directly control the contour error on the basis of the estimated contour error. The first cross-coupled control (CCC) structure for biaxial control systems was proposed by Koren [4], where the contouring accuracy is improved by feeding back the real-time estimation of contour error to each axis. Some variants [28,29] of CCC were also proposed. Since the CCC is found to be not universally successful, recently, a new method to control the contour error for corner tracking was proposed by Rahaman et al. [30], which combines the CCC with the frequency modulated interpolation (FMI). However, owing to the coupling between the tool position and orientation for five-axis machine tools, it has not been reported that the CCC can be directly adopted for five-axis machining. Unlike the CCC, another control structure, which is named task coordinate frame approach (TCFA), was proposed by Chiu and Tomizuka [10]. Since the normal error in the task coordinate frame is used to approximate the contour error, the normal error becomes the direct objective of the contouring control. Subsequently, this control structure was adopted by Sencer and Altintas [31] to control the tool tip contour error for five-axis machine tools, while the tool orientation contour error was controlled by the integral of the contour error components. Although the TCFA can be utilized for five-axis machine tools, it may increase the computational load due to the introduction of the coordinate transformation. Seeing that the effect of matched dynamics among all axes on the contouring accuracy, for multi-axis motion systems, a perfectly matched feedback control (PMFBC) was proposed by Yeh and Hsu [2], which uses stable pole-zero cancellation and complementary zeros inclusion techniques. Howerer, the PMFBC may not be achieved for five-axis machining since the models are difficult to identify accurately. By considering the contour error model of the tool center point (TCP), a five-axis servo dynamics matching method was proposed by Lin and Wu [32]. Decoupling the contour errors predicted off-line into all the drives to modify the reference position commands of each axis, a contour error pre-compensation approach for five-axis machine tools was presented by Zhang et al. [21]. By feeding back the axis components of the contour errors to the position commands with a proper proportional gain, a contour error component compensation control approach was proposed by Yang and Altintas [22]. A dual sliding mode contouring controller was proposed in our previous work [23], where the dual sliding surface including a tracking sliding surface, a contouring sliding surface and the control input, was designed separately for each axis. The contour error component control method has been used in the recent works [21–23,31]. However, the contour error components are expressed in the workpiece coordinate system, while the drive commands or tracking errors are defined in the machine coordinate system. They are directly added together, which raises a problem: when the contour error components are introduced into the controller, the contour errors instead increase in some regions of the tracking trajectory. This phenomenon is particularly noticeable in the experimental results shown in [21,31] and our previous work [23]. Obviously, it is detrimental for the actual machining operations.

Motivated by an endeavor to attack the aforementioned problems, this study proposes a new contour error estimation method for five-axis machine tools. The reference point closest to the current actual position is searched firstly, and a second-order polynomial is adopted to interpolate this reference point with its two neighboring reference points. Then, the point nearest to the actual position, which may be called foot point, can be estimated by definition. Finally, the tool tip contour error can be obtained. The tool orientation contour error is estimated by the distance ratio method, where the ratio is obtained using the actual position of the foot point between two adjacent reference points. The proposed estimation method has high accuracy while depending on only the reference points. When the contour error components are introduced into the controller, the contour errors increase instead in some regions of the tracking trajectory. In order to alleviate this problem, the contour errors are decoupled in the form of components, and a new error variable is constructed by adding a weighted contour error on the tracking error in the workpiece coordinate system. Based on this new error variable, the contouring controller can be designed simply by specifying a desired second-order error dynamics. Compared with the case without contour error control, the proposed contouring control method can reduce the contour error along the whole trajectory.

2 Modeling of contour errors of five-axis machine tools

2.1 Kinematic model for five-axis machine tools

During five-axis machining operation, the movement of the tool depends on the motion of the drives of the machine tool. Typical five-axis machine tools have three translational and two rotary drives. Here a tilting-rotary-table (TRT) type five-axis machine tool, known as the most economic [33], is

adopted as an example, as shown in Figure 2(a). The TRT type five-axis machine tool has three degrees of freedom (DOF) in the *X*-, *Y*-, and *Z*-direction and two additional rotary DOF with respect to *A*- and *C*-axis. Since the cutter location $\mathbf{P}(t)=[P_x(t), P_y(t), P_z(t)]^{\mathrm{T}}$ and orientation $\mathbf{O}(t)=[O_i(t), O_j(t), O_k(t)]^{\mathrm{T}}$, $\|\mathbf{O}(t)\|=1$ are generated from the CAD/CAM software systems, they are expressed in the workpiece coordinate system as illustrated in Figure 2(b). The actual inputs of the control system of the machine tool $\mathbf{q}(t)=[X(t), Y(t), Z(t), \theta_A(t), \theta_C(t)]^{\mathrm{T}}$ are defined in the machine coordinate system. The transformation between these two coordinate systems called kinematics modeling should be accomplished first, as illustrated in Figure 2.

Currently, the kinematics modeling can be achieved by utilizing Denavit-Hartenberg (D-H) method [33]. Then, the forward kinematics can be calculated as following:

$$\begin{bmatrix} O_i(t) \\ O_j(t) \\ O_k(t) \end{bmatrix} = \begin{bmatrix} \sin(\theta_A(t))\sin(\theta_C(t)) \\ \sin(\theta_A(t))\cos(\theta_C(t)) \\ \cos(\theta_A(t)) \end{bmatrix}, \tag{1}$$

$$\begin{bmatrix} P_x(t) \\ P_y(t) \\ P_z(t) \end{bmatrix} = \begin{bmatrix} \cos(\theta_C(t)) & \cos(\theta_A(t))\sin(\theta_C(t)) & \sin(\theta_A(t))\sin(\theta_C(t)) \\ -\sin(\theta_C(t)) & \cos(\theta_A(t))\cos(\theta_C(t)) & \sin(\theta_A(t))\cos(\theta_C(t)) \\ 0 & -\sin(\theta_A(t)) & \cos(\theta_A(t)) \end{bmatrix} \times \begin{bmatrix} X(t) \\ Y(t) \\ Z(t) \end{bmatrix} + \begin{bmatrix} -\cos(\theta_A(t))\sin(\theta_C(t)) & -\sin(\theta_A(t))\sin(\theta_C(t)) \\ 1-\cos(\theta_A(t))\cos(\theta_C(t)) & -\sin(\theta_A(t))\cos(\theta_C(t)) \\ \sin(\theta_A(t)) & 1-\cos(\theta_A(t)) \end{bmatrix} \times \begin{bmatrix} L_Y \\ L_Z \end{bmatrix}, \tag{2}$$

where L_Y and L_Z are linear offsets respectively along the *Y*- and *Z*-axis direction between the point ***P*** on the *A*-axis and the origin of the workpiece coordinate system, as illustrated in Figure 2(b). From eqs. (1) and (2), the inverse kinematics can be obtained, and then the positions of Cartesian and rotary axes can be calculated as following:

$$\begin{aligned} &\theta_A(t) = \cos^{-1}(O_k(t)), (-\pi < \theta_A(t) \le \pi), \\ &\theta_C(t) = \tan^{-1}(O_i(t), O_j(t)), (O_i(t) \ne 0, O_j(t) \ne 0), \end{aligned} \tag{3}$$

$$\begin{bmatrix} P_x(t) \\ P_y(t) \\ P_z(t) \end{bmatrix} = \begin{bmatrix} \cos(\theta_C(t)) & \cos(\theta_A(t))\sin(\theta_C(t)) & \sin(\theta_A(t))\sin(\theta_C(t)) \\ -\sin(\theta_C(t)) & \cos(\theta_A(t))\cos(\theta_C(t)) & \sin(\theta_A(t))\cos(\theta_C(t)) \\ 0 & -\sin(\theta_A(t)) & \cos(\theta_A(t)) \end{bmatrix} \times \begin{bmatrix} X(t) \\ Y(t) \\ Z(t) \end{bmatrix} + \begin{bmatrix} -\cos(\theta_A(t))\sin(\theta_C(t)) & -\sin(\theta_A(t))\sin(\theta_C(t)) \\ 1-\cos(\theta_A(t))\cos(\theta_C(t)) & -\sin(\theta_A(t))\cos(\theta_C(t)) \\ \sin(\theta_A(t)) & 1-\cos(\theta_A(t)) \end{bmatrix}$$

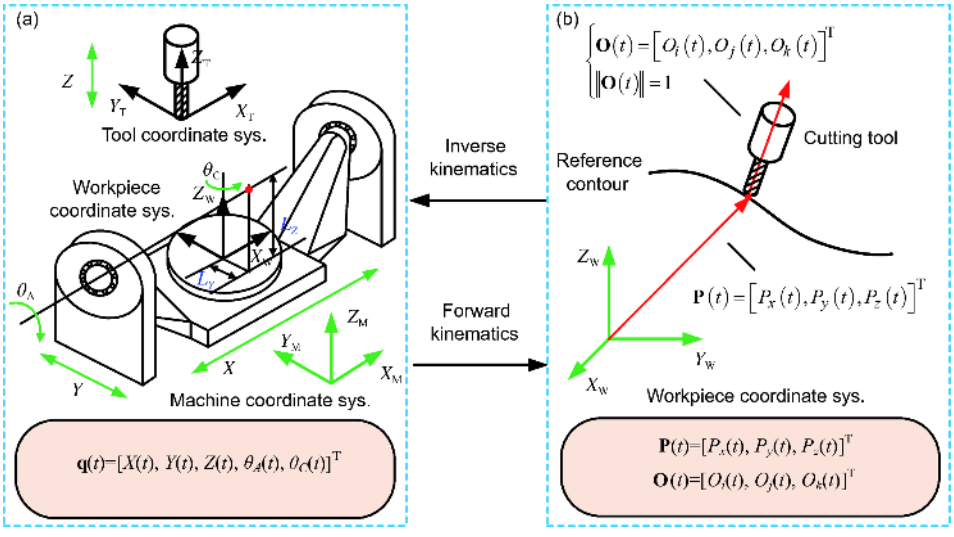

Figure 2 (Color online) Kinematics for TRT type five-axis machine tool. (a) Kinematic configuration; (b) tool path generated in the workpiece coordinate system.

$$\times\begin{bmatrix}L_Y\\L_Z\end{bmatrix}. \tag{4}$$

The first-order partial derivatives of the tool orientation with respect to the positions of rotary axes can be obtained by differentiating eq. (1), and then the orientation Jacobian $J_O(t)\epsilon\Re^{3\times2}$ can be calculated as following:

$$\mathbf{J}_O(t)=\begin{bmatrix}\cos(\theta_A(t))\sin(\theta_C(t)) & \sin(\theta_A(t))\cos(\theta_C(t))\\ \cos(\theta_A(t))\cos(\theta_C(t)) & -\sin(\theta_A(t))\sin(\theta_C(t))\\ -\sin(\theta_A(t)) & 0\end{bmatrix}, \tag{5}$$

which relates the velocities of rotary axes to the tool angular velocity of the machine as

$$\begin{bmatrix}\dot{O}_i(t)\\ \dot{O}_j(t)\\ \dot{O}_k(t)\end{bmatrix}=\mathbf{J}_O(t)\begin{bmatrix}\dot{\theta}_A(t)\\ \dot{\theta}_C(t)\end{bmatrix}. \tag{6}$$

Similar to the orientation Jacobian, the position Jacobian $J_P(t)\epsilon\Re^{3\times5}$ can also be acquired by the first-order partial derivatives of eq. (2) with respect to the positions of all drives as following:

$$\mathbf{J}_P(t)=\frac{\partial P_n(t)}{\partial q_l(t)}, n\in(x,y,z), q_l\in(X,Y,Z,\theta_A,\theta_C). \tag{7}$$

By combining the cutter location $\mathbf{P}(t)=[P_x(t),\ P_y(t),\ P_z(t)]^{\mathrm{T}}$ and orientation $\mathbf{O}(t)=[O_i(t),\ O_j(t),\ O_k(t)]^{\mathrm{T}}$, which will be adopted later for the contouring controller design, a tool pose variable can be defined as

$$\mathbf{P}_O(t)=\left[P_x(t),P_y(t),P_z(t),O_i(t),O_j(t),O_k(t)\right]^{\mathrm{T}}. \tag{8}$$

Differentiating eq. (8) with respect to the positions of all drives and considering eqs. (6) and (7), it can be shown that

$$\dot{\mathbf{P}}_O(t)=\mathbf{J}(t)\dot{\mathbf{q}}(t), \tag{9}$$

where

$$\mathbf{J}(t)=\begin{bmatrix}J_{P11} & J_{P12} & J_{P13} & J_{P14} & J_{P15}\\ J_{P21} & J_{P22} & J_{P23} & J_{P24} & J_{P25}\\ J_{P31} & J_{P32} & J_{P33} & J_{P34} & J_{P35}\\ 0 & 0 & 0 & J_{O11} & J_{O12}\\ 0 & 0 & 0 & J_{O21} & J_{O22}\\ 0 & 0 & 0 & J_{O31} & J_{O32}\end{bmatrix}, \tag{10}$$

where J_{Puv} (u=1, 2, 3, v=1, 2, 3, 4, 5) is the element in the u-th row and v-th column of the position Jacobian matrix, and J_{Ouv} (u=1, 2, 3, v=1, 2) is the element in the u-th row and v-th column of the orientation Jacobian matrix. By differentiating eq. (9), it can be shown that

$$\ddot{\mathbf{P}}_O(t)=\dot{\mathbf{J}}(t)\dot{\mathbf{q}}(t)+\mathbf{J}(t)\ddot{\mathbf{q}}(t). \tag{11}$$

Obviously, the tool pose accelerations $\ddot{\mathbf{P}}_O(t)$ is related to the drive velocities $\dot{\mathbf{q}}(t)$ and accelerations $\ddot{\mathbf{q}}(t)$ by $\mathbf{J}(t)$ and its first-order derivatives $\dot{\mathbf{J}}(t)$.

2.2 Real-time estimation of contouring errors

The five-axis contouring accuracy is affected simultaneously by the translational and rotary drives. The synchronization of the movements of tool position and orientation must be satisfied along the tool path to avoid any overcut or undercut in the machined surface. As illustrated in Figure 3, suppose that $\mathbf{P}_a$ and $\mathbf{P}_r$ are the actual and desired tool tip position, and $\mathbf{P}_f$ is the nearest tool tip position on the desired contour to the actual tool position, and $\mathbf{O}_a$, $\mathbf{O}_r$ and $\mathbf{O}_f$ are the tool orientation at the point $\mathbf{P}_a$, $\mathbf{P}_r$ and $\mathbf{P}_f$, respectively, then the tool tip contour error ε_P is the distance between $\mathbf{P}_f$ and $\mathbf{P}_a$, while the tool orientation contour error ε_O is the angular difference between $\mathbf{O}_f$ and $\mathbf{O}_a$.

To estimate the contour error as accurately as possible, it is necessary to find the point that is closest to the current actual position on the reference curve, and this point can be called foot point. For the given spline tool-path, although the accurate computation of the foot point can be performed iteratively, it may increase the computational complexity. In order to reduce the computational effort without loss of largely computational accuracy, in our previous work [23] a foot point estimation method based on the second-order Taylor expansion has been proposed, and then the tool orientation at the foot point was obtained by the linear interpolation about the curve parameter. However, it still involves the calculation of the geometric information of the curve such as the tangent, normal vectors and curve parameter, etc. Here a new estimation method is proposed, which guarantees high accuracy while depending on only the reference points. The details of the proposed new method are presented as follows.

First, by adopting the look-up table approach, the reference point $\mathbf{P}_q$ closest to the current actual position $\mathbf{P}_a$ can be obtained as shown in Figure 4(a). Since the foot point is located between $\mathbf{P}_{q-1}$ and $\mathbf{P}_q$ or $\mathbf{P}_q$ and $\mathbf{P}_{q+1}$, a second-order polynomial curve that passes through these three points $\mathbf{P}_{q-1}$, $\mathbf{P}_q$ and $\mathbf{P}_{q+1}$ can be constructed by the interpolation method. Since the reference points acquired after interpolation must have the time stamp, the tracking time t can be reasonably considered as the parameter of the polynomial. The polynomial can be described as the following form:

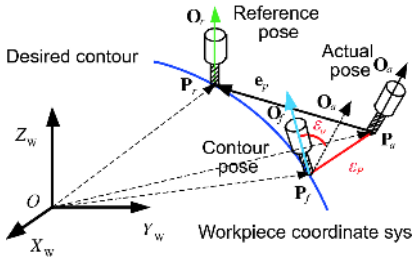

Figure 3 (Color online) Synchronized illustration for five-axis contour errors.

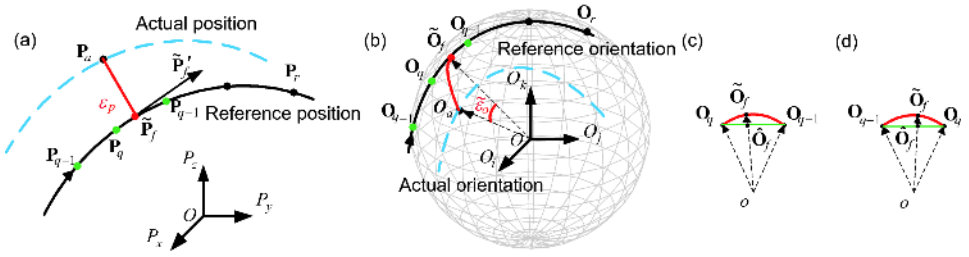

Figure 4 (Color online) Five-axis contour error estimations. (a) Tool tip contour error estimation; (b)–(d) tool orientation contour error estimation.

$$\mathbf{P} = \mathbf{P}(t), \tag{12}$$

that is

$$\begin{cases} P_x(t) = a_{2,x}t^2 + a_{1,x}t + a_{0,x}, \\ P_y(t) = a_{2,y}t^2 + a_{1,y}t + a_{0,y}, \\ P_z(t) = a_{2,z}t^2 + a_{1,z}t + a_{0,z}, \end{cases} \tag{13}$$

where $a_{m,n}$ (m=0, 1, 2, n=x, y, z) is the coefficients of the polynomial. Assuming that T_s is the sampling period, then the coordinates $(x_{t-1}, y_{t-1}, z_{t-1})$, (x_t, y_t, z_t) and $(x_{t+1}, y_{t+1}, z_{t+1})$ of the points $\mathbf{P}_{q-1}$, $\mathbf{P}_q$ and $\mathbf{P}_{q+1}$ can be expressed as

$$\begin{cases} x_{t-1} = P_x(t-T_s), \\ y_{t-1} = P_y(t-T_s), \\ z_{t-1} = P_z(t-T_s), \end{cases} \begin{cases} x_t = P_x(t), \\ y_t = P_y(t), \\ z_t = P_z(t), \end{cases} \begin{cases} x_{t+1} = P_x(t+T_s), \\ y_{t+1} = P_y(t+T_s), \\ z_{t+1} = P_z(t+T_s). \end{cases} \tag{14}$$

Rewriting eq. (14) concisely in matrix form as

$$\mathbf{AX} = \mathbf{B}, \tag{15}$$

where

$$\mathbf{A} = \begin{bmatrix} (t-T_s)^2 & t-T_s & 1 \\ t^2 & t & 1 \\ (t+T_s)^2 & t+T_s & 1 \end{bmatrix}, \mathbf{X} = \begin{bmatrix} a_{0,x} & a_{0,y} & a_{0,z} \\ a_{1,x} & a_{1,y} & a_{1,z} \\ a_{2,x} & a_{2,y} & a_{2,z} \end{bmatrix}, \tag{16}$$

$$\mathbf{B} = \begin{bmatrix} x_{t-1} & y_{t-1} & z_{t-1} \\ x_t & y_t & z_t \\ x_{t+1} & y_{t+1} & z_{t+1} \end{bmatrix}.$$

Since $\det(\mathbf{A}) = -2T_s^3$, where $\det(\cdot)$ is the determinant of the matrix, the matrix $\mathbf{A}$ is nonsingular. Then the coefficients can be obtained as

$$\mathbf{X} = \mathbf{A}^{-1}\mathbf{B}. \tag{17}$$

Second, suppose that $\tilde{\mathbf{P}}_f$ is the foot point, then the coordinate of $\tilde{\mathbf{P}}_f$ can be expressed as

$$\tilde{\mathbf{P}}_f = \left(P_x(t_f), P_y(t_f), P_z(t_f)\right), \tag{18}$$

where t_f is the time parameter of the point $\tilde{\mathbf{P}}_f$. Assume that the coordinate of $\mathbf{P}_a$ is $(P_{a,x}, P_{a,y}, P_{a,z})$, according to the definition of the foot point, the inner product between the vector consisting of the point $\mathbf{P}_a$ and $\tilde{\mathbf{P}}_f$ and the tangent vector $\tilde{\mathbf{P}}'_f$ at the point $\tilde{\mathbf{P}}_f$ should be equal to zero, that is

$$\left(P_a - \tilde{P}_f\right) \cdot \tilde{P}'_f = 0. \tag{19}$$

Further simplification of eq. (19) can be obtained as

$$bt_f^3 + ct_f^2 + dt_f + g = 0, \tag{20}$$

where

$$\begin{aligned} b &= -2\left(a_{2,x}^2 + a_{2,y}^2 + a_{2,z}^2\right), \\ c &= -3\left(a_{2,x}a_{1,x} + a_{2,y}a_{1,y} + a_{2,z}a_{1,z}\right), \\ d &= 2a_{2,x}\left(P_{a,x} - a_{0,x}\right) - a_{1,x}^2 + 2a_{2,y}\left(P_{a,y} - a_{0,y}\right) \\ &\quad - a_{1,y}^2 + 2a_{2,z}\left(P_{a,z} - a_{0,z}\right) - a_{1,z}^2, \\ g &= a_{1,x}\left(P_{a,x} - a_{0,x}\right) + a_{1,y}\left(P_{a,y} - a_{0,y}\right) + a_{1,z}\left(P_{a,z} - a_{0,z}\right). \end{aligned} \tag{21}$$

Since eq. (20) is a cubic equation about the time t_f, and it can be solved using the analytical root-finding algorithm such as Shengjin's formulas [34]. Once the time t_f is calculated, the foot point can be obtained, and then the estimated tool tip contour error can be expressed as

$$\tilde{\varepsilon}_P = \left\|\tilde{\mathbf{P}}_f - \mathbf{P}_a\right\|, \tag{22}$$

where $\|\cdot\|$ is the Euclidean norm. It can be seen that the proposed tool tip contour error estimation only depends on the information of the reference points, and it does not involve the calculation of any additional curve information. Since the local shape of the curve is approximated by the second-order polynomial curve, compared with our previous work, the proposed estimation method still has high accuracy.

Though the estimation of the tool orientation $\tilde{\mathbf{O}}_f$ at the foot point $\tilde{\mathbf{P}}_f$ has been achieved with high accuracy in our previous work, and then the tool orientation contour error $\tilde{\varepsilon}_O$ can be obtained as illustrated in Figure 4(b), it still needs the knowledge of the curve parameter. Here an improved tool orientation contour error estimation approach is proposed.

In Figure 4(b)–(d), $\mathbf{O}_{q-1}$, $\mathbf{O}_q$ and $\mathbf{O}_{q+1}$ are the known tool orientations that correspond to the reference points $\mathbf{P}_{q-1}$, $\mathbf{P}_q$ and $\mathbf{P}_{q+1}$, respectively. Suppose that $\tilde{\mathbf{O}}_f$ is the tool orientation estimated at the foot point, since the foot point is located between $\mathbf{P}_{q-1}$ and $\mathbf{P}_q$ or $\mathbf{P}_q$ and $\mathbf{P}_{q+1}$, $\tilde{\mathbf{O}}_f$must be located be-

tween $\mathbf{O}_{q-1}$ and $\mathbf{O}_q$ or $\mathbf{O}_q$ and $\mathbf{O}_{q+1}$. Suppose that $\widetilde{\mathbf{O}}_f$ is the intersection of $\widetilde{\mathbf{O}}_f$ and the line $\mathbf{O}_{q-1}\mathbf{O}_q$ or $\mathbf{O}_q\mathbf{O}_{q+1}$, then the estimated tool orientation $\widetilde{\mathbf{O}}_f$ can be acquired from the following two cases.

Case 1 (Figure 4 (c)): If the foot point is located between the point $\mathbf{P}_{q-1}$ and $\mathbf{P}_q$, the distance ratio λ can be defined as

$$\lambda = \frac{\left\|\mathbf{P}_q - \widetilde{\mathbf{P}}_f\right\|}{\left\|\mathbf{P}_q - \mathbf{P}_{q-1}\right\|}. \tag{23}$$

By utilizing the ratio, $\widetilde{\mathbf{O}}_f$ can be computed as

$$\widehat{\mathbf{O}}_f = \mathbf{O}_q + \lambda \cdot \left(\mathbf{O}_{q-1} - \mathbf{O}_q\right). \tag{24}$$

Case 2 (Figure 4(d)): If the foot point is located between the point $\mathbf{P}_q$ and $\mathbf{P}_{q+1}$, the distance ratio λ can be defined as

$$\lambda = \frac{\left\|\widetilde{\mathbf{P}}_f - \mathbf{P}_q\right\|}{\left\|\mathbf{P}_{q+1} - \mathbf{P}_q\right\|}. \tag{25}$$

By utilizing the ratio, $\widetilde{\mathbf{O}}_f$ can be computed as

$$\widehat{\mathbf{O}}_f = \mathbf{O}_q + \lambda \cdot \left(\mathbf{O}_{q+1} - \mathbf{O}_q\right). \tag{26}$$

Using vector unitization method to normalize $\widehat{\mathbf{O}}_f$, then the estimated tool orientation can be obtained as

$$\widetilde{\mathbf{O}}_f = \frac{\widehat{\mathbf{O}}_f}{\left\|\widehat{\mathbf{O}}_f\right\|}. \tag{27}$$

Therefore, the estimated tool orientation contour error illustrated in Figure 4(b) can be expressed as

$$\tilde{\varepsilon}_O = \arccos\left(\widetilde{\mathbf{O}}_f \cdot \mathbf{O}_a\right), \tag{28}$$

where $\boldsymbol{O}_a$ is the actual tool orientation.

Obviously, the tool orientation contour error is still estimated by the linear interpolation method. However, since the actual position of the foot point between $\mathbf{P}_{q-1}$ and $\mathbf{P}_q$ or $\mathbf{P}_q$ and $\mathbf{P}_{q+1}$ is utilized, compared with our previous work, the improved method does not need the information of the curve parameter.

From eqs. (19) and (22) it can be seen that, the tool tip contour error is obtained by the foot point, which is similar to the calculation of the true contour error, thus the estimated value is very close to the true value. The estimation error is mainly derived from the local approximation of the curve. For the tool orientation contour error, the distance ratio method is used. However, since the orientation differences between two adjacent reference positions are tiny, such estimation can also have high accuracy.

In order to help the design of the following contouring controller, the contour errors can be decoupled in the form of components as

$$\begin{aligned}\boldsymbol{\varepsilon} &= [\varepsilon_x, \varepsilon_y, \varepsilon_z, \varepsilon_i, \varepsilon_j, \varepsilon_k]^{\mathrm{T}} \\ &= \left[\widetilde{P}_{f,x}, \widetilde{P}_{f,y}, \widetilde{P}_{f,z}, \widetilde{O}_{f,i}, \widetilde{O}_{f,j}, \widetilde{O}_{f,k}\right]^{\mathrm{T}} \\ &- \left[P_{a,x}, P_{a,y}, P_{a,z}, O_{a,i}, O_{a,j}, O_{a,k}\right]^{\mathrm{T}},\end{aligned} \tag{29}$$

where $\widetilde{P}_{f,n}$ and $P_{a,n}$ (n=x, y, z) are the Cartesian coordinates of the foot point $\widetilde{\mathbf{P}}_f$ and the actual tool tip position $\mathbf{P}_a$, respectively. $\widetilde{O}_{f,n}$ and $O_{a,n}$ (n=i, j, k) are the spherical coordinates of the tool orientation $\widetilde{\mathbf{O}}_f$ at the foot point and the actual tool orientation $\mathbf{O}_a$, respectively.

3 Component-based contouring controller design

The simplified dynamics of a single feed drive system can be presented as illustrated in Figure 5. For five-axis machine tools, when the subscript l=X, Y, Z, A, C is adopted to denote X-, Y-, Z-, A-, C-drives, respectively, the dynamics of the five-axis machine tool can be expressed by using the following decoupled second-order differential equations as

$$\begin{aligned}&\mathbf{M}\ddot{\mathbf{q}}(t) + \mathbf{C}\dot{\mathbf{q}}(t) = \mathbf{u}(t) - \mathbf{d}(t), \\ &\mathbf{M}=\mathrm{diag}\{m_l\}, \mathbf{C} = \mathrm{diag}\{c_l\}, \mathbf{u} = \mathrm{diag}\{u_l\}, \mathbf{d} = \mathrm{diag}\{d_l\},\end{aligned} \tag{30}$$

where $\mathrm{diag}\{\cdot\}$ denotes the diagonal matrix, and u_l is the actual control voltage produced by the control law of the l-th drive, and

$$m_l = \frac{J_l}{K_{al}K_{tl}R_{gl}}, c_l = \frac{B_l}{K_{al}K_{tl}R_{gl}}, d_l = \frac{1}{K_{al}K_{tl}}T_{dl}, \tag{31}$$

where K_{al} and K_{tl} are the current amplifier and servo motor constant of the l-th drive, respectively. J_l and B_l are the inertia and viscous damping of the l-th drive, respectively. R_{gl} is the reduction ratio of the l-th drive. T_{dl} is the external disturbance of the l-th drive, which includes the friction, backlash as well as the cutting forces, etc. For the convenience of writing, the symbol t will be omitted in the following formulas. Using eq. (30), the drive accelerations $\ddot{\mathbf{q}}$ can be obtained in compact form as

$$\ddot{\mathbf{q}} = \mathbf{M}^{-1}(\mathbf{u} - \mathbf{d} - \mathbf{C}\dot{\mathbf{q}}). \tag{32}$$

Substituting eq. (32) into eq. (11), the drive dynamics then can be mapped to the actual tool pose $\mathbf{P}_O$ as follows:

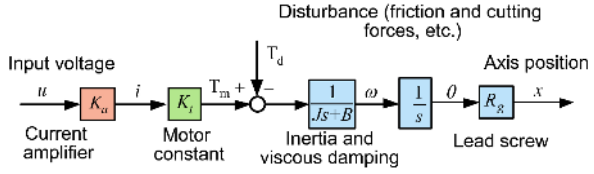

Figure 5 (Color online) Simplified linear dynamics of a single feed drive system.

$$\ddot{\mathbf{P}}_O = \dot{\mathbf{J}}\dot{\mathbf{q}} + \mathbf{J}\mathbf{M}^{-1}(\mathbf{u} - \mathbf{d} - \mathbf{C}\dot{\mathbf{q}}). \tag{33}$$

Assuming that the reference tool pose is

$$\mathbf{P}_{O,\mathrm{ref}} = \left[P_{x,\mathrm{ref}}, P_{y,\mathrm{ref}}, P_{z,\mathrm{ref}}, O_{i,\mathrm{ref}}, O_{j,\mathrm{ref}}, O_{k,\mathrm{ref}}\right]^{\mathrm{T}}, \tag{34}$$

then the tracking errors in the workpiece coordinate system can be expressed as

$$\mathbf{e} = [e_x, e_y, e_z, e_i, e_j, e_k]^{\mathrm{T}} = \mathbf{P}_{O,\mathrm{ref}} - \mathbf{P}_O. \tag{35}$$

By substituting eq. (33) into eq. (35), the tracking error dynamics in the workpiece coordinate system can be expressed as

$$\ddot{\mathbf{e}} = \ddot{\mathbf{P}}_{O,\mathrm{ref}} - \dot{\mathbf{J}}\dot{\mathbf{q}} - \mathbf{J}\mathbf{M}^{-1}(\mathbf{u} - \mathbf{d} - \mathbf{C}\dot{\mathbf{q}}). \tag{36}$$

Since the goal of tracking control is only to reduce the tracking error, which does not necessarily mean the improvement of the contour accuracy, direct contour error control is certainly needed. Meanwhile, the tracking control and contouring control are to make the tool actual pose close to the reference pose and contour pose, respectively, thus they should be considered simultaneously in the workpiece coordinate system. By adding a weighted contour error on the tracking error in the workpiece coordinate system, a new error variable can be constructed as

$$\tilde{e} = \mathbf{e} + \boldsymbol{\rho}\boldsymbol{\varepsilon}, \tag{37}$$

where $\boldsymbol{\rho}$=diag$\{\rho_x, \rho_y, \rho_z, \rho_i, \rho_j, \rho_k\}$ is the weight coefficient matrix. A desired second-order error dynamics can be specified simply as follows:

$$\ddot{\tilde{e}} + K_v\dot{\tilde{e}} + K_p\tilde{e} = 0, \tag{38}$$

where $\mathbf{K}_v$=diag$\{K_{vx}, K_{vy}, K_{vz}, K_{vi}, K_{vj}, K_{vk}\}$ and $\mathbf{K}_p$=diag$\{K_{px}, K_{py}, K_{pz}, K_{pi}, K_{pj}, K_{pk}\}$ are the positive velocity and position gain matrices, respectively. Since the vibration property of a control system may affect the machined surface quality, the control system is desirable to have critically damped dynamics. Hence the controller gains are set as

$$K_{vn} = 2\omega_n,\ K_{pn} = \omega_n^2,\ n \in (x, y, z, i, j, k), \tag{39}$$

where ω_n is the closed-loop pole of the control system, which can be determined by the designer. Differentiating eq. (37) and substituting the results into eq. (38), for the five drive axes the control law $\mathbf{u} = [u_X, u_Y, u_Z, u_A, u_C]^{\mathrm{T}}$ can be obtained as

$$\begin{aligned}\mathbf{u} = \mathbf{M}\mathbf{J}^{+}\Big[&\ddot{\mathbf{P}}_{O,\mathrm{ref}} + \mathbf{K}_v\dot{\mathbf{P}}_{O,\mathrm{ref}} + \mathbf{K}_p\mathbf{P}_{O,\mathrm{ref}} + \boldsymbol{\rho}\left(\ddot{\boldsymbol{\varepsilon}} + \mathbf{K}_v\dot{\boldsymbol{\varepsilon}} + \mathbf{K}_p\boldsymbol{\varepsilon}\right)\\ &-\mathbf{K}_v\dot{\mathbf{P}}_O - \mathbf{K}_p\mathbf{P}_O - \dot{\mathbf{J}}\dot{\mathbf{q}}\Big] + \mathbf{C}\dot{\mathbf{q}} + \mathbf{d},\end{aligned} \tag{40}$$

where $\mathbf{J}^{+}$ is the Moore-Penrose pseudoinverse of the Jacobian matrix $\mathbf{J}$, which can be computed as $\mathbf{J}^{+} = (\mathbf{J}^{\mathrm{T}}\mathbf{J})^{-1}\mathbf{J}^{\mathrm{T}}$. $\dot{\boldsymbol{\varepsilon}}$ and $\ddot{\boldsymbol{\varepsilon}}$ are the first- and second-order derivatives of the contour error $\boldsymbol{\varepsilon}$, respectively. The entries $\dot{\varepsilon}_n$ and $\ddot{\varepsilon}_n$ (n=x, y, z, i, j, k) in $\dot{\boldsymbol{\varepsilon}}$ and $\ddot{\boldsymbol{\varepsilon}}$, respectively, can be calculated utilizing the backward difference formula as following:

$$\dot{\varepsilon}_n = \frac{3\varepsilon_{n,0} - 4\varepsilon_{n,-1} + \varepsilon_{n,-2}}{2h_n}, \tag{41}$$

$$\ddot{\varepsilon}_n = \frac{2\varepsilon_{n,0} - 5\varepsilon_{n,-1} + 4\varepsilon_{n,-2} - \varepsilon_{n,-3}}{h_n^2}, \tag{42}$$

where $\varepsilon_{n,-m}$ (m=0, 1, 2, 3) is the n-axis component of the contour error in the m-th previous sampling time that corresponds to the current time. h_n is the sampling interval.

From eq. (38) it can be seen that the proposed controller shown in eq. (40) is exponentially stable. Obviously, the contouring performance will be good when using large value of $\boldsymbol{\rho}$. However, it is difficult to determine the range of $\boldsymbol{\rho}$ which can guarantee stability from theoretical analysis. Since the contour error is considered as the disturbance of tracking control, even if we only care about the contouring errors, the large value of $\boldsymbol{\rho}$ may lead to system instablity, which instead worsens the contouring performance. Thus, under the condition of system stabiltiy, the maximum value of $\boldsymbol{\rho}$ can be determined by trial and error from zero, and then the range of $\boldsymbol{\rho}$ can be obtained.

Since the sharp corners contain high frequency content, the accuracy of the proposed controller degrades at the sharp corners of the tracking trajectory. However, by the optimal feedrate planning, feedforward control action and friction compensation, the contouring accuracy at the sharp corners can be maintained well.

4 Implementation and experimental results

The proposed contour error estimation and contouring control methods are validated on a real time TRT five-axis experimental system, as shown in Figure 6. A computer with the VC++ 2012 and MATLAB software is adopted to plan the feedrate, calculate the interpolation and design the controller, and it also can communicate with the dSPACE DS1103 controller board through the ControlDesk software and the fiber bus hardware. For the five-axis machine tool, all feed axes are driven by Yaskawa AC servo motors which have the current control loop. For the X-, Y- and Z-axes, all the motors are combined with a 10 mm pitch^{-1} leadscrew, while the motors of the A- and C- axes are coupled with the harmonic reducers. The reduction ratios of these reducers are 100:1. The encoders of all axes, which are located in the back of the servo motors and with a resolution of 10000 pulses rev^{-1}, are used for the position sensing of the feed systems. Then, by differentiating the positions with respect to the time and using the appropriate low-pass filter to remove high frequency noise, the velocities of five axes can be obtained. There exist two linear offsets in the kinematic transformation as shown in eqs. (2) and (4), and their values are given by measurement as L_Y=0 mm and L_Z= 41 mm. The dynamics parameters of each drive are identified

using the method proposed by Erkorkmaz and Altintas [35], and the results are shown in Table 1.

4.1 Verification of the contour error estimations

Several air cutting experiments are conducted for the verification of the contour error estimations. Since in the existing literature involving five-axis contour error estimations, our previous work [23] may be the most accurate, the method proposed now is compared with it for the discrepancies between the estimated contour errors and the true ones. The true contour errors are acquired off-line by computing the shortest distance between the actual and the reference tool paths. Two trajectories are used, and one is the blade-shaped curve, the other is the fan-shaped curve mentioned in ref. [36]. By adopting the appropriate feedrate planning method, these two tool paths can be obtained with an interpolation period of 1 ms and a maximum tangential feed rate of 80 mm s^{-1}. The blade-shaped trajectory and its drive commands are illustrated in Figure 7, and its experimental results

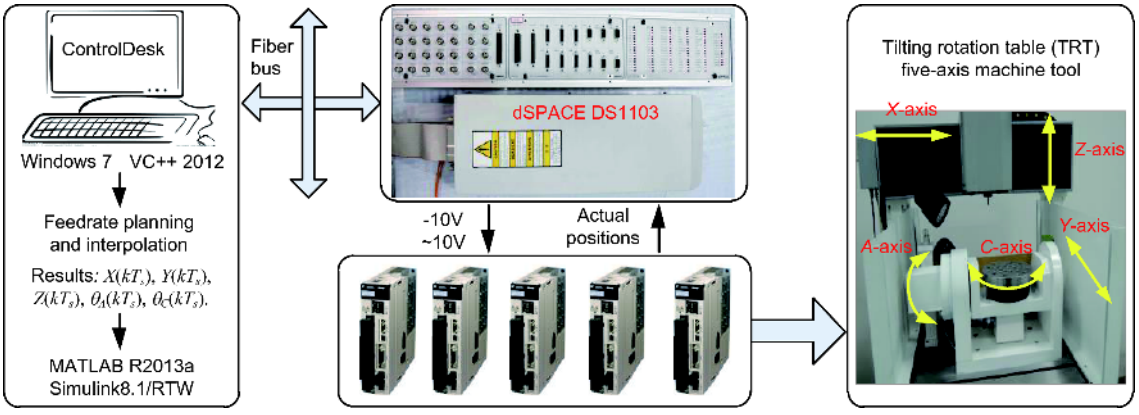

Figure 6 (Color online) Five-axis experimental system.

Table 1 Dynamics parameters of each drive

Parameters	*X*-axis	*Y*-axis	*Z*-axis	*A*-axis	*C*-axis
m (V s^2 m^{-1} or V s^2 rad^{-1})	0.2146	0.2863	0.1567	0.1101	0.0721
c (V s m^{-1} or V s rad^{-1})	1.994	1.131	1.464	0.4001	0.3871

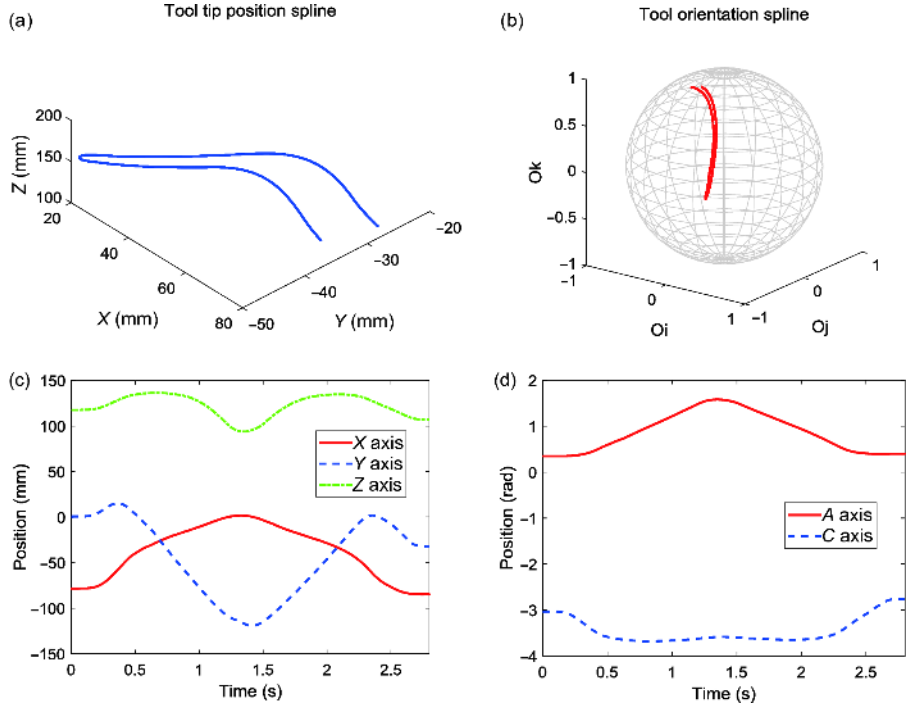

Figure 7 (Color online) The blade-shaped trajectory and drive commands for each axis.

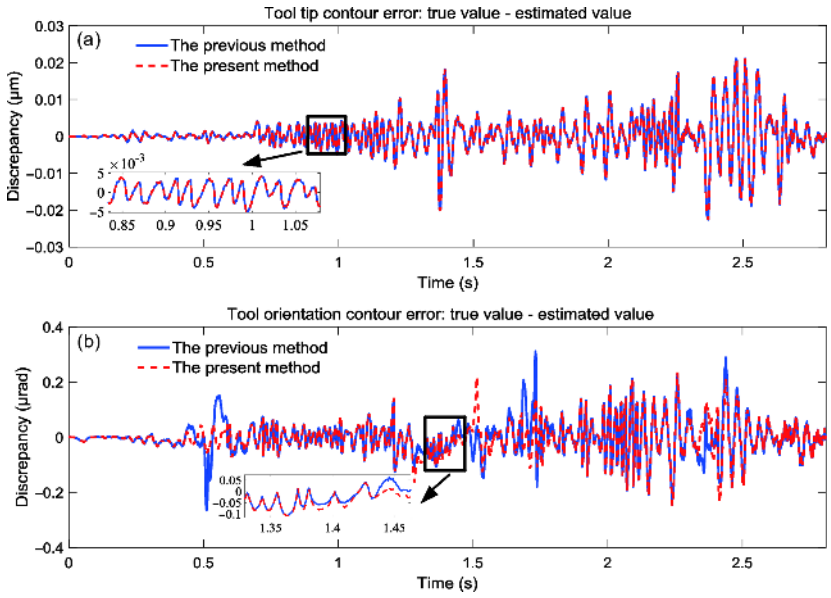

Figure 8 (Color online) The estimated contour errors and their discrepancies with the true values for the blade-shaped trajectory.

are given in Figure 8.

The results demonstrate that, whether the tool tip contour error or tool orientation contour error, the estimated contour errors by the method proposed now have very small discrepancies with the true ones. Meanwhile, when compared with our previous work, the method proposed now has a similar tool tip contour error estimation accuracy and a little higher tool orientation contour error estimation accuracy. The curvature of the tool tip position spline for the blade-shaped trajectory is given in Figure 9, it can be seen that although there exist some large curvature positions, the estimated tool tip contour errors are still very small within 0.05 μm, which demonstrates the estimation method proposed now is robust to curvature variance.

The fan-shaped trajectory and its drive commands are illustrated in Figure 10, and its experimental results are given in Figure 11. The results demonstrate the same conclusions similar to the blade-shaped trajectory, which shows the estimation method proposed now is trajectory type independent. The reasons for Figures 8 and 11 can be given as follows: for our previous work, a second-order Taylor expansion is used to estimate the tool tip contour error, while the tool orientation contour error is obtained by the ratio about the curve parameter difference; for the method proposed now, a second-order polynomial interpolation is adopted to estimate the tool tip contour error, while the tool orientation contour error is acquired by the ratio about the distance of the foot point. Therefore, the method proposed now still has a similar tool tip contour error estimation accuracy with our previous work, and has a little higher tool orientation contour error estimation accuracy than our previous work.

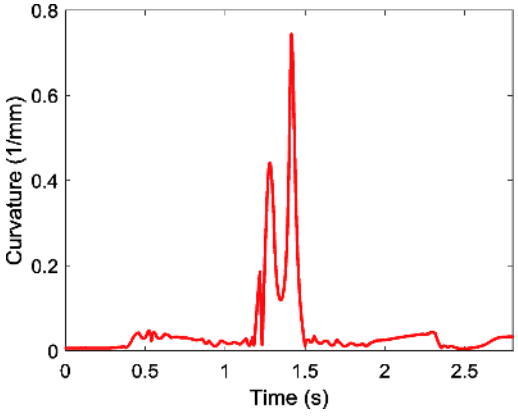

Figure 9 (Color online) Curvature of the position spline of blade-shaped trajectory.

Obviously, the method proposed now does not involve the calculation of the geometric information of the curve such as the tangent, normal vectors and curvature, etc., but only introduces the calculation of the inverse of a 3×3 matrix. Meanwhile, for our previous work and the method proposed now, both of which are achieved using M code, the mean computing time are 0.04326 and 0.02574 ms, respectively. Therefore, the computational efficiency of the method proposed now is superior to that of our previous work from the qualitative and quantitative analysis.

4.2 Verification of the contouring controller

The fan-shaped trajectory is used to validate the proposed contouring controller. Table 2 gives the controller parameters, which are appropriately tuned, and the experimental

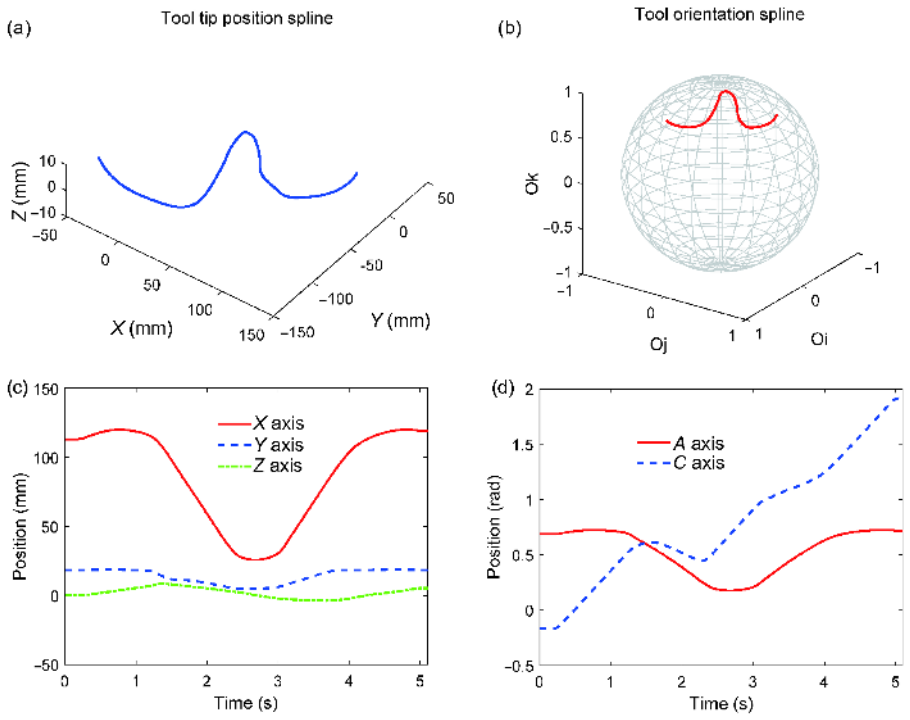

Figure 10 (Color online) The fan-shaped trajectory and drive commands for each axis.

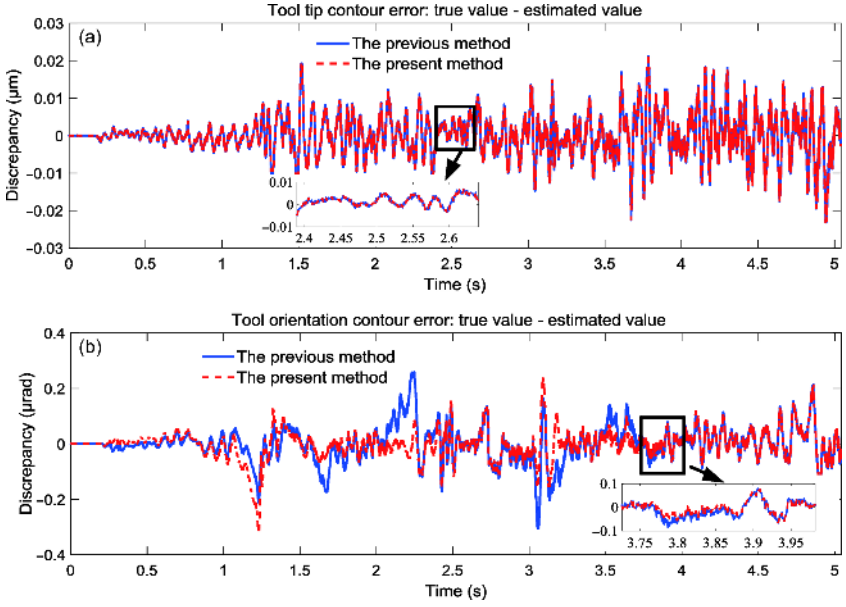

Figure 11 (Color online) The estimated contour errors and their discrepancies with the true values for the fan-shaped trajectory.

results are presented in Figure 12. It can be seen that, when the nonlinear kinematics of five-axis machine tool is considered in the controller, the tracking error and contouring error are uniformly defined in the workpiece coordinate system. Based on the newly constructed error variable, the contouring control action is introduced by the weight ($\boldsymbol{\rho}$=0.6). Compared with the traditional controller ($\boldsymbol{\rho}$=0), the proposed control method can effectively achieve the global contour error reduction. The problem is that the contour errors increase instead when introducing the contouring control action can be alleviated, which is helpful for the actual machining. The experimental data illustrated in Figure 12 is further analyzed quantitatively as shown in Table 3, which reveals that the maximum and mean contour errors have an

Table 2 Controller parameters

Parameters	*x*-axis	*y*-axis	*z*-axis	*i*-axis	*j*-axis	*k*-axis
K_v(m s^{-1} or rad s^{-1})	75.40	75.40	75.40	31.42	31.42	31.42
K_p(m s^{-2} or rad s^{-2})	8882.64	8882.64	8882.64	3947.84	3947.84	3947.84

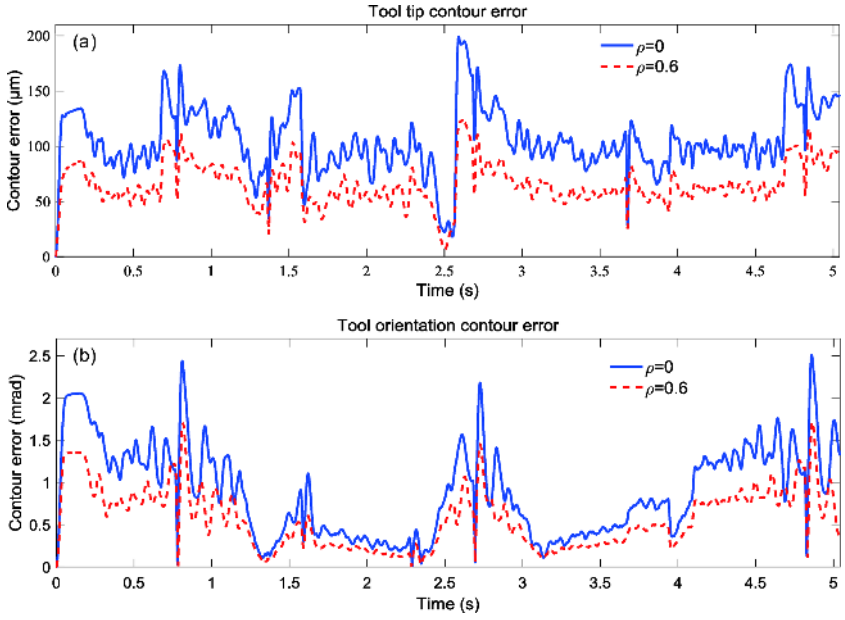

Figure 12 (Color online) Experimental results of the proposed contouring controller.

Table 3 Comparison of experimental contour errors

Selections	Tool tip contour error		Tool orientation contour error	
	Max. (μm)	Mean (μm)	Max. (mrad)	Mean (mrad)
Without contour action (**ρ**=0)	199.0575	104.5749	2.5049	0.8876
With contour action (**ρ**=0.6)	123.9285	65.3905	1.7120	0.5708

obvious decrease.

5 Conclusions

Since high accuracy contour error estimation and direct contour error control can improve the contouring accuracy during machining, an effective contouring controller with a real-time high-accuracy contour error estimation for five-axis machine tools is proposed in this paper. First, the contour errors are estimated by the second-order polynomial interpolation and the distance ratio method. Compared with existing studies, the proposed estimation method only depends on the reference points and still has high accuracy. Then, the contour errors are decoupled in the form of components, and the contouring controller is obtained by specifying a desired second-order error dynamics about a new error variable. This error variable is constructed by adding a weighted contour error on the tracking error in the workpiece coordinate system. Different from existing contour error component control methods, since the nonlinear kinematics of five-axis machine tool is considered, the proposed contouring controller can effectively reduce the contour error along the whole trajectory. Some experimental results obtained on a TRT five-axis experimental system validate the effectiveness of the proposed contour error estimation method and the contouring controller.

This work was supported by the National Natural Science Foundation of China (Grant Nos. 51535004 & 91748114).

1 Sencer B, Altintas Y, Croft E. Modeling and control of contouring errors for five-axis machine tools—Part I: Modeling. J Manuf Sci Eng, 2009, 131: 031006
2 Yeh S S, Hsu P L. Perfectly matched feedback control and its integrated design for multiaxis motion systems. J Dyn Syst-T ASME, 2004, 126: 547–557
3 Erkorkmaz K, Altintas Y. High speed CNC system design. Part III: High speed tracking and contouring control of feed drives. Int J Mach Tool Manu, 2001, 41: 1637–1658
4 Koren Y. Cross-coupled biaxial computer control for manufacturing

systems. J Dyn Syst-T ASME, 1980, 102: 265
5 Yeh S S, Hsu P L. Estimation of the contouring error vector for the cross-coupled control design. IEEE-ASME T Mech, 2002, 7: 44–51
6 Zhu L M, Zhao H, Ding H. Real-time contouring error estimation for multi-axis motion systems using the second-order approximation. Int J Mach Tool Manu, 2013, 68: 75–80
7 Yang J Z, Li Z X. A novel contour error estimation for position loop-based cross-coupled control. IEEE-ASME T Mech, 2011, 16: 643–655
8 Chuang H Y, Liu C H. A model-referenced adaptive control strategy for improving contour accuracy of multiaxis machine tools. IEEE T Ind Appl, 1992, 28: 221–227
9 El Khalick M A, Uchiyama N. Contouring controller design based on iterative contour error estimation for three-dimensional machining. Robot Cim-Int Manu, 2011, 27: 802–807
10 Chiu G T C, Tomizuka M. Contouring control of machine tool feed drive systems: A task coordinate frame approach. IEEE Trans Contr Syst Tech, 2001, 9: 130–139
11 Shi R, Lou Y J. A novel contouring error estimation for three-dimensional contouring control. IEEE Robot Autom Lett, 2017, 2: 128–134
12 Yao B, Hu C X, Wang Q F. An orthogonal global task coordinate frame for contouring control of biaxial systems. IEEE-ASME T Mech, 2012, 17: 622–634
13 Wu J H, Xiong Z H, Ding H. Integral design of contour error model and control for biaxial system. Int J Mach Tool Manu, 2015, 89: 159–169
14 Erkorkmaz K, Altintas Y. High speed contouring control algorithm for CNC machine tools. ASME Dyn Syst Contr Div, 1998, 64: 463–469
15 Huo F, Xi X C, Poo A N. Generalized Taylor series expansion for free-form two-dimensional contour error compensation. Int J Mach Tool Manu, 2012, 53: 91–99
16 Conway J R, Ernesto C A, Farouki R T, et al. Performance analysis of cross-coupled controllers for CNC machines based upon precise real-time contour error measurement. Int J Mach Tool Manu, 2012, 52: 30–39
17 Chen S L, Wu K C. Contouring control of smooth paths for multiaxis motion systems based on equivalent errors. IEEE Trans Contr Syst Technol, 2007, 15: 1151–1158
18 Ghaffari A, Ulsoy A G. Dynamic contour error estimation and feedback modification for high-precision contouring. IEEE-ASME T Mech, 2016, 21: 1732–1741
19 Lo C C. A tool-path control scheme for five-axis machine tools. Int J Mach Tool Manu, 2002, 42: 79–88
20 El Khalick M A, Uchiyama N. Estimation of tool orientation contour errors for five-axismachining. Robot Cim-Int Manuf, 2013, 29: 271–277
21 Zhang K, Yuen A, Altintas Y. Pre-compensation of contour errors in five-axis CNC machine tools. Int J Mach Tool Manu, 2013, 74: 1–11
22 Yang J X, Altintas Y. A generalized on-line estimation and control of five-axis contouring errors of CNC machine tools. Int J Mach Tool Manu, 2015, 88: 9–23
23 Li X F, Zhao H, Zhao X, et al. Dual sliding mode contouring control with high accuracy contour error estimation for five-axis CNC machine tools. Int J Mach Tool Manu, 2016, 108: 74–82
24 Tomizuka M. Zero phase error tracking algorithm for digital control. J Dyn Syst-T ASME, 1987, 109: 65–68
25 Masory O. Improving contouring accuracy of NC/CNC systems with additional velocity feed forward loop. J Eng Ind, 1986, 108: 227–230
26 Xi X C, Zhao W S, Poo A N. Improving CNC contouring accuracy by robust digital integral sliding mode control. Int J Mach Tool Manu, 2015, 88: 51–61
27 Chiu G T C, Tomizuka M. Coordinated position control of multi-axis mechanical systems. J Dyn Syst-T ASME, 1998, 120: 389–393
28 Zhao H, Zhu L M, Ding H. Cross-coupled controller design for triaxial motion systems based on second-order contour error estimation. Sci China Tech Sci, 2015, 58: 1209–1217
29 Chen W, Wang D D, Geng Q, et al. Robust adaptive cross-coupling position control of biaxial motion system. Sci China Tech Sci, 2016, 59: 680–688
30 Rahaman M, Seethaler R, Yellowley I. A new approach to contour error control in high speed machining. Int J Mach Tool Manu, 2015, 88: 42–50
31 Sencer B, Altintas Y. Modeling and control of contouring errors for five-axis machine tools—Part II: Precision contour controller design. J Manuf Sci Eng, 2009, 131: 031007
32 Lin M T, Wu S K. Modeling and improvement of dynamic contour errors for five-axis machine tools under synchronous measuring paths. Int J Mach Tool Manu, 2013, 72: 58–72
33 Jung Y H, Lee D W, Kim J S, et al. NC post-processor for 5-axis milling machine of table-rotating/tilting type. J Mater Process Tech, 2002, 130-131: 641–646
34 Fan S J. A new extracting formula and a new distinguishing means on the one variable cubic equation. Nat Sci J Hainan Teach Coll, 1989, 2: 91–98
35 Erkorkmaz K, Altintas Y. High speed CNC system design. Part II: Modeling and identification of feed drives. Int J Mach Tool Manu, 2001, 41: 1487–1509
36 Fleisig R V, Spence A D. A constant feed and reduced angular acceleration interpolation algorithm for multi-axis machining. Comput-Aided Des, 2001, 33: 1–15